

Article

# Distribution of Selected Trace Elements in the Bayer Process <sup>†</sup>

Johannes Vind <sup>1,2,\*</sup> , Alexandra Alexandri <sup>2</sup>, Vicky Vassiliadou <sup>1</sup> and Dimitrios Panias <sup>2,\*</sup>

<sup>1</sup> Department of Continuous Improvement and Systems Management, Aluminium of Greece Plant, Metallurgy Business Unit, Mytilineos S.A., Agios Nikolaos, 32003 Viotia, Greece; vicky.vassiliadou@alhellas.gr

<sup>2</sup> School of Mining and Metallurgical Engineering, National Technical University of Athens, Iroon Polytechniou 9, Zografou Campus, 15780 Athens, Greece; aalexandri@metal.ntua.gr

\* Correspondence: johannes.vind@alhellas.gr (J.V.); panias@metal.ntua.gr (D.P.); Tel.: +30-210-7722184 (J.V.); +30-210-772-2276 (D.P.)

† This paper is the written, extended and updated version of the oral presentation entitled as “Distribution of Trace Elements Through the Bayer Process and its By-Products”, presented in the 35th International Conference and Exhibition ICSOBA-2017 which was held in Hamburg, Germany from 2–5 October 2017; Vind, J.; Vassiliadou, V.; Panias, D. Distribution of trace elements through the Bayer process and its by-products. In Proceedings, Travaux 46; Hamburg, Germany, 2–5 October 2017; pp. 255–267; <https://icsoba.org/sites/default/files/2017papers/Alumina%20Papers/AA14%20-%20Distribution%20of%20Trace%20Elements%20Through%20the%20Bayer%20Process%20and%20its%20By%20Products.pdf> (accessed on 23 March 2018).

Received: 9 April 2018; Accepted: 3 May 2018; Published: 8 May 2018



**Abstract:** The aim of this work was to achieve an understanding of the distribution of selected bauxite trace elements (gallium (Ga), vanadium (V), arsenic (As), chromium (Cr), rare earth elements (REEs), scandium (Sc)) in the Bayer process. The assessment was designed as a case study in an alumina plant in operation to provide an overview of the trace elements behaviour in an actual industrial setup. A combination of analytical techniques was used, mainly inductively coupled plasma mass spectrometry and optical emission spectroscopy as well as instrumental neutron activation analysis. It was found that Ga, V and As as well as, to a minor extent, Cr are principally accumulated in Bayer process liquors. In addition, Ga is also fractionated to alumina at the end of the Bayer processing cycle. The rest of these elements pass to bauxite residue. REEs and Sc have the tendency to remain practically unaffected in the solid phases of the Bayer process and, therefore, at least 98% of their mass is transferred to bauxite residue. The interest in such a study originates from the fact that many of these trace constituents of bauxite ore could potentially become valuable by-products of the Bayer process; therefore, the understanding of their behaviour needs to be expanded. In fact, Ga and V are already by-products of the Bayer process, but their distribution patterns have not been provided in the existing open literature.

**Keywords:** Bayer process; trace elements; vanadium; gallium; rare earth elements; lanthanum; yttrium; scandium; karst bauxite; bauxite residue; red mud

## 1. Introduction

The ever-increasing growth in the electronics industry, the production of light-weight electric vehicles as well as devices for generating renewable energy have imposed an accelerating demand for specific raw materials such as the rare earth elements (REEs) [1–3]. Several economic regions like the European Union, Japan or USA have identified raw materials that are categorised as “critical”, relating to their supply risk and economic importance [1,4]. The search for new sources for critical

metals has encouraged research work in, amongst others, the alumina industry, in which the caustic process liquor as well as its by-product known as bauxite residue or red mud are prospective sources of certain critical metals [5–8].

More than 50 chemical elements existing typically in bauxites occur in higher concentrations than 1 mg/kg [9] and, therefore, can be considered as trace elements. The alumina industry is particularly interested in the bauxite trace elements for the following reasons: (1) some of them (such as vanadium—V) are undesired impurities that might end up in the product and, therefore, their fractionation through the process must be controlled [10]; (2) some of them (such as gallium—Ga—and in some cases scandium—Sc) can be extracted mainly as a by-product of the primary alumina industry [6,11–13]; (3) some of them (such as beryllium—Be) are considered hazardous from environmental and occupational health points of view [14]. Therefore, keeping track on the fate of trace elements within the Bayer process is very important for the best plant performance and the desired purity of products.

In the present work we set our focus on the Bayer process related trace elements that have a prospect or already possess an existing value of being or becoming a profitable by-product. It is well-known that Ga is worldwide mainly produced as a by-product of Bayer process [8,15] and V can also be recovered as vanadium sludge during the production of alumina [7,16]. There exists a growing interest in the extraction of the relatively valuable REEs and Sc from bauxite residue by exploiting various hydrometallurgical or combined pyro- and hydrometallurgical routes [5–7,11,17,18]. In addition, the demand for these metals has been increasing steadily and further increase is projected in the future [1,3,15].

For a better clarity in further discussion, it should be noted that REEs are a group of chemical elements known as the lanthanides as well as yttrium (Y). Sc is also considered often as a REE, but there is no conclusive consensus in this question. Based on the chemical properties, REEs are usually divided to light REEs (LREE, lanthanum to europium) and heavy REEs (HREE, gadolinium to lutetium and Y) [19], which is also the official IUPAC definition.

To name a few applications where some of the metals discussed in the present paper are used, it can be mentioned that Ga is dominantly used in semi-conductors as well as in light emitting diodes [8,20]. The primary use of V is in the steel industry, where this alloying metal provides grain refinement and hardenability [21]. A wide matrix of applications exists for the REEs, such as strong permanent magnets used in electric motors, catalysts, batteries, phosphors, polishing and many more [19]. The interest is growing in the so far relatively scarcely used Sc, which can be utilised to produce light-weight aluminium (Al) alloys beneficial in the aerospace industry. Another rapidly growing field of Sc applications is in solid oxide fuel cells, which accounts now for about 90% of the use of this metal [1,22].

Regardless of the long history of Ga research in alumina industry [9,12,23], it is not easy to retrieve published data of the distribution of Ga in the Bayer process. It has been emphasised that this missing gap in the accessible information has affected the compilation of worldwide resource estimation exercises, as there is no source available that relates the known Ga concentrations with actual material mass flows in the Bayer process [8,15]. Similar gaps exist for V, chromium (Cr), arsenic (As) and the REEs. For instance, Deady et al. [24] have identified this gap in the available literature and recommend to assess the enrichment of REEs from bauxite to its residues by relating the actual source and resulting materials. Some information can be retrieved about the distribution patterns of lanthanum (La) and Sc in the Bayer process [25], but given the date of this study (1981) it is useful to update and build new knowledge upon that existing study. For the rest of the elements considered in this work, at most the fractionation indexes between bauxite and derived residue or merely concentrations can be found [26–28], and those are also often given based on lab-scale experiments [29,30]. Comprehensive descriptions exist that provide the behaviour and distribution patterns of other bauxite trace elements like molybdenum (Mo), zinc (Zn) [31], Be [14,32], thorium (Th) and uranium (U) [33] as well as mercury (Hg) in the Bayer process [34,35]. It is of high interest to examine in particular the karst/diasporic

bauxite trace element distribution in the Bayer process, because these types of bauxites are relatively more enriched in trace elements compared to lateritic/gibbsitic bauxites [36,37].

The aim of this work is therefore to establish the distribution patterns of selected trace elements (Ga, V, As, Cr, REEs, Sc) in the Bayer process and its by-products by formulating mass balance models of the named elements based on a case study. The results of the present work can be further utilised as one of the sources for compiling global resource estimations, Bayer-process-related resource estimations, planning of by-product production from Bayer process materials, etc.

## 2. Materials and Methods

The Bayer process is a cyclic method that utilises sodium hydroxide leaching of bauxite ore to produce technically pure alumina (>98.3%  $\text{Al}_2\text{O}_3$ ) [38–41]. Aluminium of Greece plant (Metallurgy Business Unit, Mytilineos S.A.; hereafter denoted as AoG) uses a set of processing conditions that are known in the industrial sector as high temperature digestion (HTD). These conditions ( $T > 250\text{ }^\circ\text{C}$ , elevated pressure) are dictated by the utilisation of mainly karst bauxite, in which primary alumina-containing minerals are diaspore ( $\alpha\text{-AlO(OH)}$ ), digested mostly at  $>250\text{ }^\circ\text{C}$  in the presence of lime) and boehmite ( $\gamma\text{-AlO(OH)}$ ), digested mostly at  $>240\text{ }^\circ\text{C}$  that dissolve less readily than the more commonly exploited gibbsite mineral ( $\text{Al(OH)}_3$ , digested mostly at  $140\text{--}150\text{ }^\circ\text{C}$ ) [9,42,43].

A simplified flow diagram of AoG's process is shown in Figure 1. Because Parnassos-Ghiona bauxite in its natural position is situated between limestones, it is necessary to remove the unwanted limestone from the ore that is inevitably partly mined as a contaminant together with bauxite. Limestone, mineralogically composed mainly of calcite, is removed by heavy media separation (HMS) in ferrosilicon slurry [44,45], also referred as “decalcitation” (sic) process in the literature [44]. This operation unit is shown in Figure 1 as “HMS”, marked by a dotted line, because it is not strictly a part of the conventional Bayer process. The primary output of this unit is mixed karst bauxite (also the main input to the Bayer process, 73% of total bauxite mass) and secondary output is “decalcitation residue”. Karst bauxite is ground in the presence of concentrated leach liquor to achieve granulometry  $<315\text{ }\mu\text{m}$  and the resulting suspension is pre-heated to about  $180\text{ }^\circ\text{C}$ . Digestion of the karst bauxite suspension is performed at about  $255\text{ }^\circ\text{C}$  and a pressure of about  $5.8\text{--}6.0\text{ MPa}$  for approximately one hour. To increase the productivity of the Bayer process, AoG also utilises an optimisation step that is termed as the “sweetening” process. In the “sweetening” process, lateritic/gibbsitic bauxite is digested at a lower temperature after the digestion of karst/diasporic bauxite. Lateritic bauxite suspension passes through a pre-desilication step with a residence time of about 24 h, to allow the formation of desilication products (sodalite and cancrinite) and to avoid the problems of reactive silica (i.e., kaolinite) during digestion. In the case of AoG, lateritic bauxite suspension is introduced to the main karst bauxite slurry in the appropriate flash stage after the HTD of karst bauxite suspension. Lime is added to the process during HTD as a reaction catalyst, as well as during causticisation step that reduces soda losses and as a filter aid during the security filtration of pregnant liquor after the settling stage (liquor “polishing”) [44,46]. From the leached effluent slurry after digestion, the solid fraction is separated as residue slurry or red mud (bauxite residue in the suspended form) by settling and washing. To obtain de-watered bauxite residue that helps to reduce the losses of soda and eases the stacking as well as further utilisation of residue, AoG makes use of the plate and frame filter pressing of the initial residue slurry after the settling and washing unit [7]. The clear pregnant liquor, rich in sodium aluminate, passes to the next processing step where crystalline aluminium hydroxide ( $\text{Al(OH)}_3$ ) is precipitated. Precipitation is initiated by the introduction of aluminium hydroxide seed crystals. The spent liquor after precipitation unit is concentrated in the evaporation unit, to create the necessary sodium hydroxide concentration level for the next processing cycle. Aluminium hydroxide, which is the final product of the Bayer process, is calcined at  $>1000\text{ }^\circ\text{C}$  to produce anhydrous alumina ( $\text{Al}_2\text{O}_3$ ) [38,39]. Sometimes, the Bayer process is divided into the “red side” to denote the units where bauxite and its residue are present, and to “white side” to indicate the stages after residue removal (clarification) until precipitation and evaporation stages [40,47].

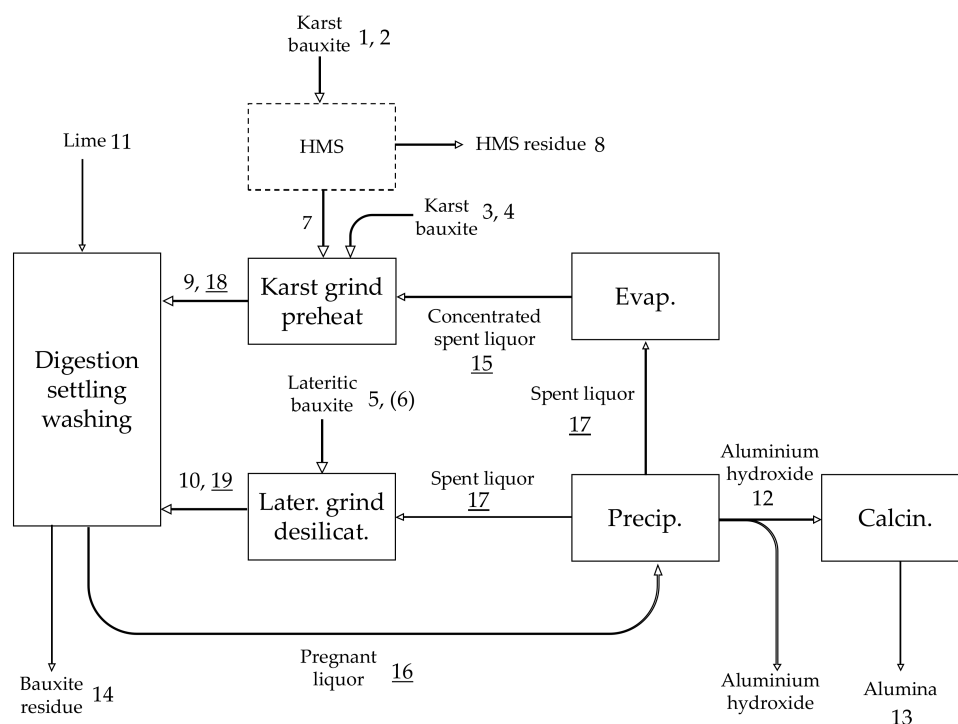


**Figure 1.** Simplified flowsheet of the Bayer process. Numbers indicate the sampled materials, whilst underlined numbers refer to samples obtained in liquor form. Numbers correspond to Table 1. HMS: Heavy media separation.

### 2.1. Sampling and Technological Data

Sampling took place over a three-day period and materials were collected from key points in the process flow sheet to provide a snapshot of the whole process. The precondition of such sampling procedure is that all the input constituents should appear in the output materials of the process and sampled output material corresponds to the sampled input material. The sampling points are shown in Figure 1, and sample descriptions are detailed in Table 1. AoG uses largely two types of bauxite feed: locally mined karst (diasporic/boehmitic) bauxite and imported lateritic (gibbsitic) bauxite. The Greek karst bauxite samples originate from the Parnassos-Ghiona B3 stratigraphic horizon, which is the youngest and most exploited horizon of the deposit [48]. A minor amount of B2 stratigraphic horizon Parnassos-Ghiona bauxite was also used at the time of sampling, but the exploitation of this material is currently suspended. More details about the Parnassos-Ghiona deposit can be found for example from Dedy et al. [24]. Another minor source of karst bauxite at the time of sampling was diasporic bauxite from Turkey, Milas area. The lateritic bauxites used at AoG originate from Brazil (Porto Trombetas) [49] and Ghana (Awaso), while only Brazilian bauxite was processed in the period of sampling campaign.

Bauxite samples were collected from the one-tonne test batches to provide the best representation of the feed material. Bayer liquors, aluminium hydroxide, alumina and lime samples were collected from the appropriate sampling points according to the internal protocols of AoG. A composite sample of bauxite residue was collected after the filter pressing of the residues. Bauxite residue from AoG is known to have a relatively stable REEs and Sc concentration (8% variation in 15 years), known from the long-term research experience related to this material [6]. Fresh sodium hydroxide addition to the process was negligible during the sampling period and was therefore excluded from the analysis. Process data for both solid and the liquid mass flows were acquired for the same period as the sampling took place.

**Table 1.** Description of the sampled materials.

Material	No.	Code	Description		
Input bauxite	Karst/diasporic	1	DD-BX	Parnassos-Ghiona bauxite from B3 horizon. Extracted by company Delphi-Distomon S.A., a subsidiary of Mytilineos S.A. In the plant jargon it is termed as “Delphi-Distomo” bauxite. This material is subjected to limestone removal before the Bayer process.	
		2	ST-BX	Parnassos-Ghiona bauxite from B3 horizon. Extracted by S&B Industrial Minerals S.A. In the plant jargon it is termed as “standard” bauxite. This material is subjected to limestone removal before the Bayer process.	
		3	HS-BX	Parnassos-Ghiona bauxite from horizon B2. It represents a minor input (1%) to the process. At present day, it is no longer exploited.	
		4	TU-BX	Bauxite from Turkey, western Taurides range and Milas area.	
	Lateritic/gibbsitic	5	TR-BX	Bauxite from Brazil, Porto Trombetas deposit. It represents the main input of lateritic bauxite to the process (21% of total bauxite input). Input of lateritic bauxite alters between this (Porto Trombetas) and Ghanaian (Awaso) bauxite.	
		6	GH-BX	Bauxite from Ghana, Awaso deposit. At the time of sampling, this material was not processed.	
		HMS unit	7	DC-BX	Mixed karst/diasporic bauxite, from which limestone is separated (“decalcitated”). Inputs to this unit are DD-BX and ST-BX. It represents the main bauxite input (73% of total bauxite input) to the Bayer process as a mixture of karst bauxite from two different mining locations that exploit B3 horizon Parnassos-Ghiona bauxite.
			8	DC-RE	HMS residue. Limestone residue that is separated from Parnassos-Ghiona B3 horizon bauxite. Besides limestone, contains also a significant proportion of rejected bauxite material.
Intermediate materials/additives	9	BF-DG	Solid fraction of karst bauxite slurry, from grinding and preheating units of karst bauxite.		
	10	SW-DS	Solid fraction of lateritic/gibbsitic bauxite slurry from pre-desilication unit.		
	11	CA-OX	Lime, CaO.		
Products/by-products	12	HY-AL	Aluminium hydroxide, Al(OH) <sub>3</sub> , output from precipitation unit.		
	13	CA-AL	Calcined alumina, Al <sub>2</sub> O <sub>3</sub> , output from calcination unit.		
	14	RM-FP	Bauxite residue after the filterpressing of residue slurry.		
<b>Liquid Samples</b>					
Liquors	15	CL	Concentrated spent liquor, from the output of evaporation unit, routed to karst bauxite grinding.		
	16	PL	Pregnant liquor, from the outlet of settling and security filtration.		
	17	SL	Spent liquor, from the outlet of precipitation. Largest proportion is routed to evaporation and a small proportion to lateritic bauxite grinding.		
Slurries	18	BF	Liquid phase from grinding and preheating units of karst bauxite, corresponds to sampling point 9 and solid sample “BF-DG”.		
	19	SW	Liquid phase from grinding and desilication unit of lateritic bauxite, corresponds to sampling point of 10 “SW-DS”.		

## 2.2. Analytical Methods

Solid samples were prepared for the analysis using standard techniques (drying, crushing, splitting, grinding, pulverising). Elemental compositions of the samples were determined by a combination of techniques listed in Table 2. Lithium borate fusion was chosen as the appropriate method prior to inductively coupled plasma mass spectrometry (ICP-MS) that ensures with high efficiency the total dissolution of bauxite and bauxite residue mineral matrix [29,50]. Instrumental neutron activation analysis (INAA) has been outlined as a good analytical technique for determining trace element concentrations in bauxite and bauxite residue as it is a non-destructive method and does not require any sample pre-treatment. Also, chemical interferences such as the matrix effect are avoided. The negative property of INAA is, however, that it is a relatively slow technique and not all chemical elements can be measured simultaneously [29,51]. The specifications of applying INAA in analysing geological materials, as practiced by Activation Laboratories Ltd., are given by Hoffman [52]. The quality of the trace element analysis was assessed by measuring certified bauxite reference material BX-N [53,54] with both methods, ICP-MS and INAA. INAA measurements were also verified with certified reference material DMMAS 120.

Bayer liquors were prepared for analyses either by (1) simply dilution, (2) acidification with concentrated HNO<sub>3</sub> [55], or (3) dewatering the liquors to obtain dry pulps of the liquor (Table 2). The latter method also provides a guarantee that trace constituents are not precipitated from the liquid phase during sample preparation. Besides, dewatering enhances the concentration of each component contained in the sample. Analysis of La and Sc in Bayer process solid as well as liquid samples was exercised previously by Derevyankin et al. [25].

## 2.3. Compiling of the Mass Balance

The results from chemical analysis were used in combination with mass flow data of the plant and normalised to the mass of produced aluminium hydroxide (on dry and calcined basis) according to Equation (1). The mass balance approach to describe trace element distribution was based on the method given by Papp et al. [31]. Original mass flow data was corrected only for the output units of “grinding and preheating of karst bauxite” and “grinding and desilication of lateritic bauxite”, assuming a constant Fe<sub>2</sub>O<sub>3</sub> total mass in solids [31]:

$$C = \frac{c \times m_1}{m_2}, \quad (1)$$

where:

- C: product-normalised concentration of trace element, mg/kg;
- c: measured concentration of trace element in solid, mg/kg; or liquid, mg/L;
- m<sub>1</sub>: mass flow of material on dry basis, kg/d; or liquor flow m<sup>3</sup>/d;
- m<sub>2</sub>: mass flow of aluminium hydroxide on dry calcined basis, kg/d.

**Table 2.** Analytical methods and preparation techniques used for the determination of trace elements in Bayer process solid and liquid samples.

	Abbreviation	Method	Preparation and Specifications
Solid samples	XRF-st	X-ray fluorescence, standardised (Perform'X, Thermo Fisher Scientific™, Waltham, MA, USA)	Fusion of solids with Li <sub>2</sub> B <sub>4</sub> O <sub>7</sub> /LiBO <sub>2</sub> (66:33) flux, sample to flux ratio 1:11 [56]. Standardised with appropriate standard materials.
	ICP-MS	Inductively coupled plasma mass spectrometry (Xseries 2, Thermo Fisher Scientific™, Waltham, MA, USA)	Fusion of solids with Li <sub>2</sub> B <sub>4</sub> O <sub>7</sub> /LiBO <sub>2</sub> (66:33) flux, sample to flux ratio 1:20, glass bead dissolved in 10% <i>v/v</i> nitric acid.
	INAA	Instrumental neutron activation analysis (Activation Laboratories Ltd., Ancaster, ON, Canada)	About 2 g of sample is inserted in a polyethylene vial [52].
	titr.	Thermometric acid-base titration (855 Robotic Titrosampler, Metrohm, Herisau, Switzerland)	Details given in method description [57].
Liquor samples	AAS	Atomic absorption spectrophotometer (2100, PerkinElmer, Waltham, MA, USA)	Appropriate dilution with deionised water.
	ICP-MS	Inductively coupled plasma mass spectrometer (specified above)	Sample is diluted with deionised water and then acidified with concentrated nitric acid while gently heating the sample in proportions 1:10:1, additional dilutions are made [55].
	ICP-OES	Inductively coupled plasma optical emission spectrometer (Optima 8000, PerkinElmer, Waltham, MA, USA)	Sample is diluted with deionised water and then acidified with concentrated nitric acid while gently heating the sample in proportions 1:10:1, additional dilutions are made [55].
	INAA	Instrumental neutron activation analysis (specified above)	Dewatering of liquor until the creation of dry pulps (Büchi Syncore, vacuum pump Büchi V-700, controller Büchi V-850; Flawil, Switzerland). Then, about 2 g of sample is inserted in a polyethylene vial.
	XRF	X-ray fluorescence, no standardisation, semi-quantitative (Xepos, Spectro, Kleve, Germany)	Dewatering of liquor until the creation of dry pulps (specified above).
	UV	UV Photometer (Cary 60 UV-Vis, Agilent, Santa Clara, CA, United States)	Acidification with conc. HCl and dilution with deionised water in proportions 1:3:20; only for analysing Fe.

### 3. Results and Discussion

The main and trace element compositions of the analysed solid materials are presented in Supplementary Tables S1 and S2. Analysis of the different bauxites supports the existing knowledge that karst bauxites are more enriched in certain trace elements compared to lateritic bauxites (Supplementary Table S2) [37]. The most prominent trace elements in all analysed bauxites and in derived residue are Cr and V. Among the REEs, Ce is always the most abundant metal in all the materials where the REEs are present. This is in accordance with the review and a case study of REEs in Greek Parnassos-Ghiona diasporic bauxite and derived residues, where the positive anomaly of Ce is always noted [24].

Bayer liquor from various production stages is relatively enriched in the concentration of Ga, V, As and K (Table 3, Supplementary Table S3). Ga, V, As and K concentrations in various Bayer plants are relatively well known, while K is considered highly soluble in the process liquors and Ga, V as well as As medium soluble [10]. Note that the concentration of some analytes, like Ga and V, is higher in the spent liquor compared to pregnant liquor. This is because the total volume of spent liquor is smaller than the total volume of pregnant liquor and therefore the concentrations appear higher. At the same time, the mass balances of these elements are in equilibrium, as explained further (Section 3.1). The same accounts for the concentration of total caustic. Mo was also accumulated to process liquor, but the behaviour and mass balance of this element in Bayer process is already given by Papp et al. [31]. Detectable concentrations of Cr and Ni are also present in Bayer liquor, but these metals are not particularly accumulated into Bayer liquor compared to their concentration in bauxite feed. Other metals, such as Ce, La or Y that were of high interest within the scope of this study, do not occur in dissolved form in Bayer liquor in detectable concentrations (Table 3). This is to be expected as the REEs are not predicted to have soluble species in highly alkaline conditions (pH > 14) [58,59], which is further supported by the mineralogical observations indicating the REEs remain in solid forms during the Bayer digestion [60]. For the case of Sc, INAA found its levels being <0.05 mg/L, which is in accordance with Suss et al. who report that Sc concentration in Bayer liquor remains <1 mg/L [13]. Bayer liquor also contains low concentrations of U (~1 mg/L), which is in accordance with previously known facts [33]. It is interesting to note that 20–30 mg/L concentration of tungsten (W) was also found in process liquors by INAA and XRF. Previous studies that have compared W concentrations in bauxite and derived residue have indicated a depletion of W in bauxite residue compared to bauxite feed, suggesting that current detection of W in Bayer liquor is realistic [29,61].

**Table 3.** Composition of Bayer process pregnant (PL) and spent (SL) liquors. Extended overview of Bayer process liquors composition is available in Supplementary Table S3.

Sample	Al <sub>2</sub> O <sub>3</sub> *	Na <sub>2</sub> O **	As	Br	Ca	Ce	Cr	Fe	Ga	Gd	K
	g/L	g/L	mg/L	mg/L	mg/L	mg/L	mg/L	mg/L	mg/L	mg/L	g/L
	titr.	titr.	INAA	INAA	AAS	ICP-MS	ICP-MS	UV	ICP-OES	ICP-MS	AAS
PL	192.2	159.4	110.8	33.6	14.9	<0.04	1.4	9.6	267.2	<0.04	13.7
SL	108.6	171.7	99.6	31.4	16.5	<0.04	1.3	3.4	279.7	<0.04	13.8
	<b>La</b>	<b>Mg</b>	<b>Mo</b>	<b>Ni</b>	<b>Sc</b>	<b>Si</b>	<b>Th</b>	<b>U</b>	<b>V</b>	<b>W</b>	<b>Y</b>
	mg/L	mg/L	mg/L	mg/L	mg/L	mg/L	mg/L	mg/L	mg/L	mg/L	mg/L
	ICP-MS	AAS	INAA	AAS	INAA	AAS	INAA	ICP-MS	ICP-OES	INAA	ICP-MS
PL	<0.04	<0.1	318	4.8	<0.05	544	<0.1	1.28	295.2	27	<0.04
SL	<0.04	<0.1	273	<4	<0.05	520	<0.1	1.27	314.7	21	<0.04

\* The aluminate content of the liquor, expressed as Al<sub>2</sub>O<sub>3</sub> [62]. \*\* Total caustic, the sum of the free Na(OH) and Na bound with sodium aluminate, expressed as Na<sub>2</sub>O [62].

Based on the preceding information about trace element concentrations in process liquors, we divided the mass distribution description of the trace elements into two main categories. The first one describes the metals (or metalloids) that accumulate to Bayer liquor or dissolve sparingly (V, Ga,

As, Cr) while the second one describes the metals for which the distribution is controlled only by solid materials (REEs and Sc).

Full data describing the distribution and mass balance inventory of all analysed trace elements is given in Supplementary Tables S4–S6. Processing steps are divided into seven principal units: (I) heavy media separation (HMS), (II) grinding and preheating of karst bauxite, (III) grinding and pre-desilication of lateritic bauxite, (IV) digestion, settling and washing, (V) precipitation, (VI) evaporation and (VII) calcination. Overall mass balance is summarised in “internal balance” which includes the process liquors in addition to solids and “external balance” that includes only solid materials input and output. For the metals which do not occur in process liquors, units V–VII are omitted, because the metal concentrations relating to those units were below detection limits (which are specified in Table S3).

### 3.1. Metals (and Metalloids) that Accumulate to Liquor

There was insignificant difference in the Ga concentrations when comparing lateritic and karst bauxites (Supplementary Table S2). This is in line with the report by U.S. Geological Survey, where they concluded a similar presence of Ga in karstic and lateritic bauxites. They summarise the world’s average Ga concentration in all analysed bauxite deposits as being 57 mg/kg [63], which is comparable to the present analysis of 57–66 mg/kg in all currently analysed bauxites. Concentrations are said to be ranging from 12–52 mg/kg Ga with an average of 40 mg/kg in bauxite districts of Greece and Turkey [63].

Gallium possesses a close relation to Al and therefore occurs prevalently in Al-minerals. Similar properties include atomic radius, trivalent oxidation state, tetrahedral or octahedral coordination and amphotericity [20,64]. The mass distribution of Ga is mainly controlled by process liquors (Figure 2). During bauxite digestion, Ga is released from aluminium-bearing minerals like gibbsite, boehmite and diaspore [20]. The Ga digestion reaction is described by Equation (2) [9]:

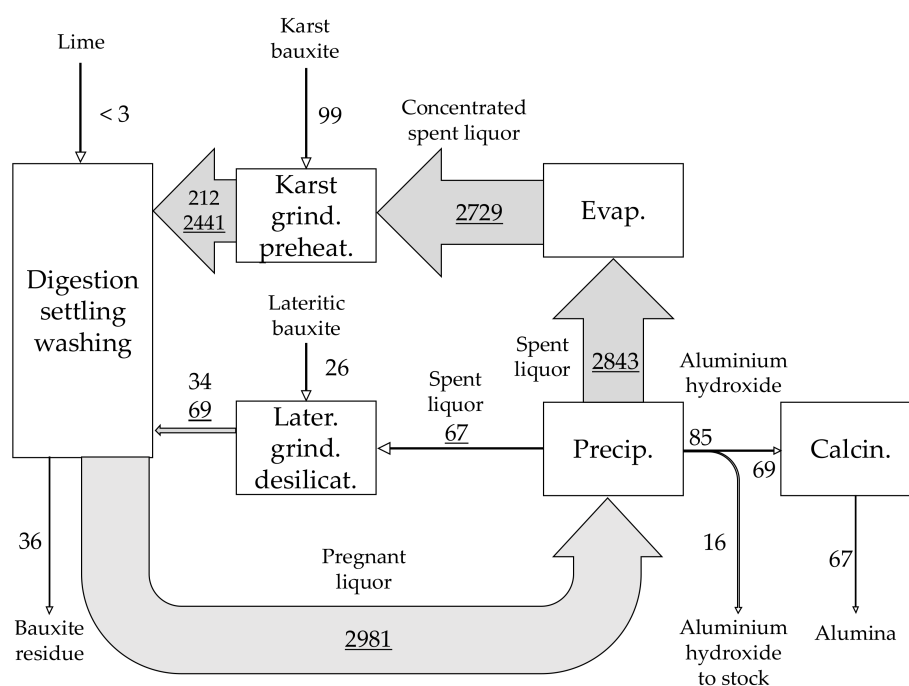
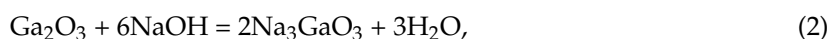


**Figure 2.** Mass distribution of Ga (mg/kg) normalised to mass of aluminium hydroxide produced, based on ICP-MS (solids) and ICP-OES (liquors) data.

Ga accumulates in process liquors, achieving saturation at levels exceeding 300 mg/L. This is about the average of that reported across earlier publications (60–600 mg/L Ga), yet typically shown values remain between 100–200 mg/L Ga [65–70]. The present Ga saturation levels are prospective for economic extraction given that Frenzel et al. suggest a conservative cut-off concentration for profitable production of Ga from process liquor being 240 mg/L [8]. Ga is about 25 times enriched into pregnant liquor compared to bauxite input. Even though the highest concentration of Ga was detected in concentrated spent liquor, the highest relative amount of Ga (allowing for volumetric changes from gibbsite precipitation and liquor evaporation) was found in pregnant liquor. This is because freshly leached Ga in digestion is present in pregnant liquor, while some Ga is precipitated along with gibbsite during precipitation and so removed from the concentrated spent liquor stream.

From the pregnant liquor, 68% of Ga entering the process is precipitated with aluminium hydroxide, resulting in the concentration of 85 mg/kg. This impurity, however, has no adverse effect on the quality of smelter grade alumina [9]. A smaller proportion of 29% reports to bauxite residue (36 mg/kg on product-normalised basis). The mass difference between the entering and exiting portion of Ga is negligible (3%). Note that the normalised concentration of Ga in liquid fraction decreases from spent liquor to concentrated spent liquor and then to the slurry after preheating stage. In the latter, the decrease of concentration in liquid fraction is accompanied by the simultaneous increase in the solid fraction. Since this is a systematic observation occurring also in the distribution of other trace elements, it will be discussed further in the text.

For the purposes of theoretical modelling of Ga distribution, Hudson [12] has indicated, and Frenzel et al. [8] have applied the partitioning of Ga as 35% going to bauxite residue and 65% to hydrate product [8,12]. From this analysis, the partitioning is more in line with that reported by Figueiredo et al. [65] with 30% of Ga going to bauxite residue, and 70% to hydroxide product, although they do not refer to the source of their data [65]. This case study therefore supports the literature that suggests about 70% of bauxite Ga is digested in the Bayer process, and this part is subsequently precipitated into aluminium hydroxide. About 30% of Ga is separated from the process with bauxite residue [65].

Almost twice as much V is contained in the karst bauxite (336–650 mg/kg) compared to the lateritic bauxite (201–258 mg/kg). Given the different proportions of bauxites in the feed, the major input of V is therefore from karst bauxite (87%). Mass distribution of V is given based on XRF-st data since it provided considerably better fit in the mass balance model compared to ICP-MS data (Figure 3).

The mass distribution of V is again mainly regulated by process liquors, where the concentration of V exceeds 400 mg/L in concentrated spent liquor. This is in accordance with the range of V saturation levels in Bayer liquors reported elsewhere in publications (100–2800 mg/L V) [10,65,69,71]. Authier-Martin et al. refer to earlier studies indicating that V is about 30% soluble during Bayer digestion [9]. Compared to bauxite feed on alumina normalised basis, V is enriched in pregnant liquor up to 4 times in this study. In process liquors, V appears in the form of  $\text{VO}_4^{3-}$  [71]. This impurity is unwanted in hydroxide and metal production due to its known property of decreasing the electric conductivity of metallic Al, causing a green hue in fused Al, and the scale it can form in the piping of a Bayer refinery when precipitated from the liquor in the cooler parts of the circuit [9,71,72]. The removal of V from process liquors is a side benefit of process lime addition. V precipitates as calcium vanadate, as an impurity in tri-calcium aluminate ( $\text{Ca}_3\text{Al}_2(\text{OH})_{12}$ ), or as  $\text{Na}_7(\text{VO}_4)_2\text{F}\cdot 19\text{H}_2\text{O}$  [71,73,74]. Our study as well as the regular monitoring in the plant materials did not detect any V in the aluminium hydroxide product (<10 mg/kg). Therefore, lime addition that mainly reduces soda losses among other beneficial effects [46], is simultaneously providing a way to remove excess V from the Bayer cycle and preventing V precipitation to product. In the existing case study, V is separated from the process and is accumulated in the bauxite residue.

The input of As to the system from lateritic bauxite (3%) is negligible compared to karst bauxite (97%). Once again, the accumulation of As to the liquor-based circuit is evident, as seen from the

diagram in Figure 4. The saturation of As to process liquor is achieved at about 130 mg/L concentration. In earlier studies, As has been detected in the alkaline liquor of bauxite residue suspension as well as in Bayer liquors [10,75]. Teas and Kotte have classified As as a medium soluble impurity in the Bayer process with a similar behaviour to V [10], which is evident also from this case study.

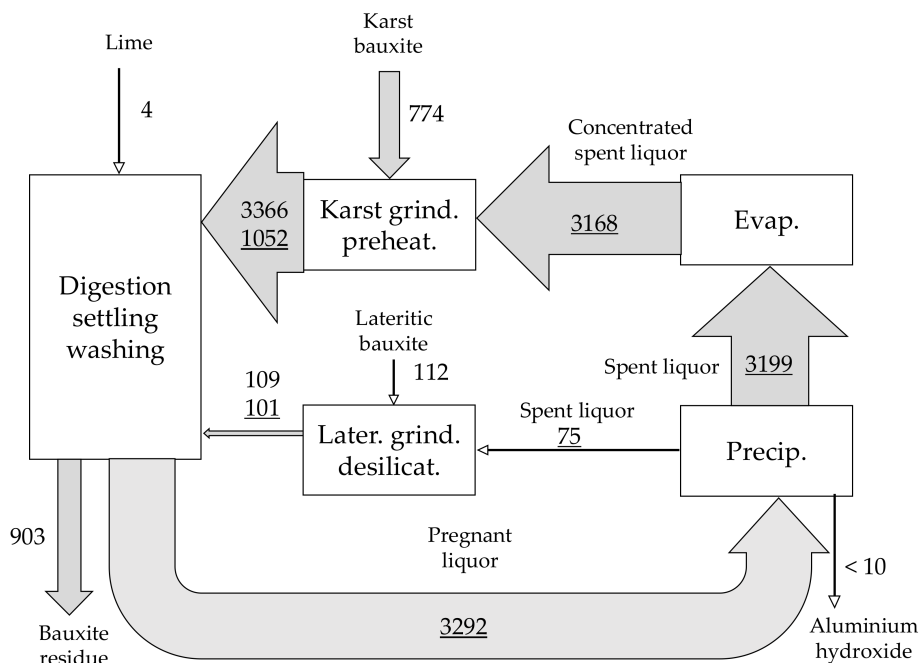


**Figure 3.** Mass distribution of V (mg/kg) normalised to mass of aluminium hydroxide produced, based on XRF-st and ICP-OES data.

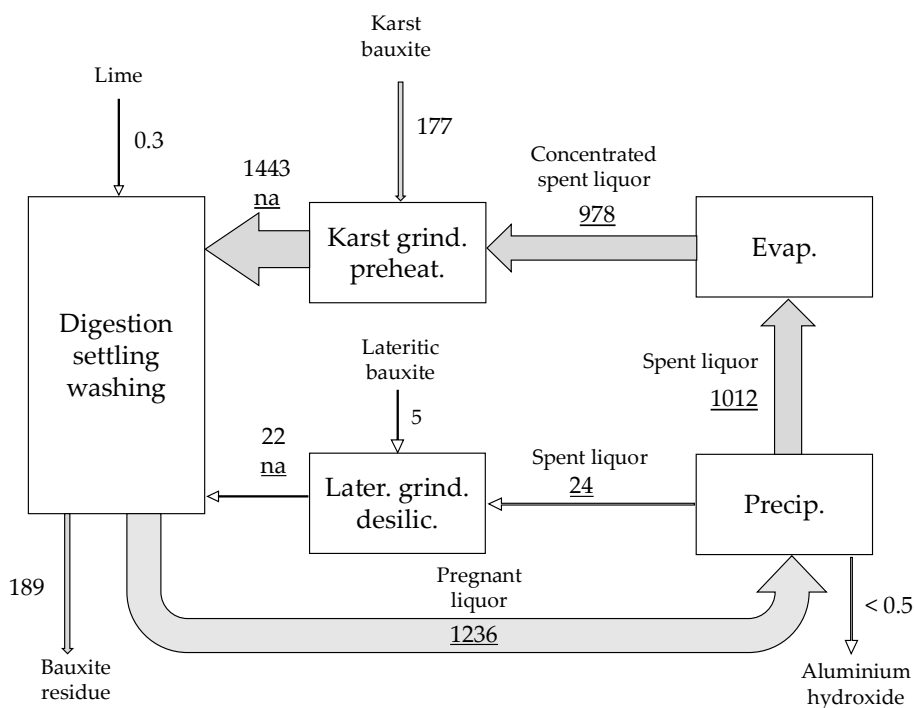


**Figure 4.** Mass distribution of As (mg/kg) normalised to mass of aluminium hydroxide produced, based on ICP-MS (solids) and INAA (liquors) data.

Higher than usual discrepancies in the input and output masses of As in different units are noted compared to other analysed elements. This could be an indication of the need to further develop analytical techniques relating to As in Bayer process materials. However, it is clear that dissolved As must exist in the system when we observe the “karst bauxite grinding and preheating” unit. It is apparent from there that As concentration increases significantly when comparing the solids entering and exiting the unit. This implies that the entering of As to solid fraction must originate from the concentrated spent liquor. In any case, in the end of the processing cycle, all of the As in found in bauxite residue and in the context of available detection limits is not shown to be present in aluminium hydroxide product (<0.5 mg/kg).

The majority of Cr input (95%) originates from karst bauxite. A minor fraction of Cr, about one percent of input, can be dissolved into process liquor giving rise to a concentration of 1.4 mg/L (Figure 5). During precipitation, Cr was not detected to enter product (<5 mg/kg), or it does in a very small quantity (~2 mg/kg), as could be suggested from difference in the balance of precipitation stage and the small deficiency (one percent) of Cr mass in the output material. An earlier study has pointed out a 5 mg/kg concentration of Cr in hydroxide product [26]. All the quantity of Cr that entered to the process is found in bauxite residue as the sole output carrier of this metal.

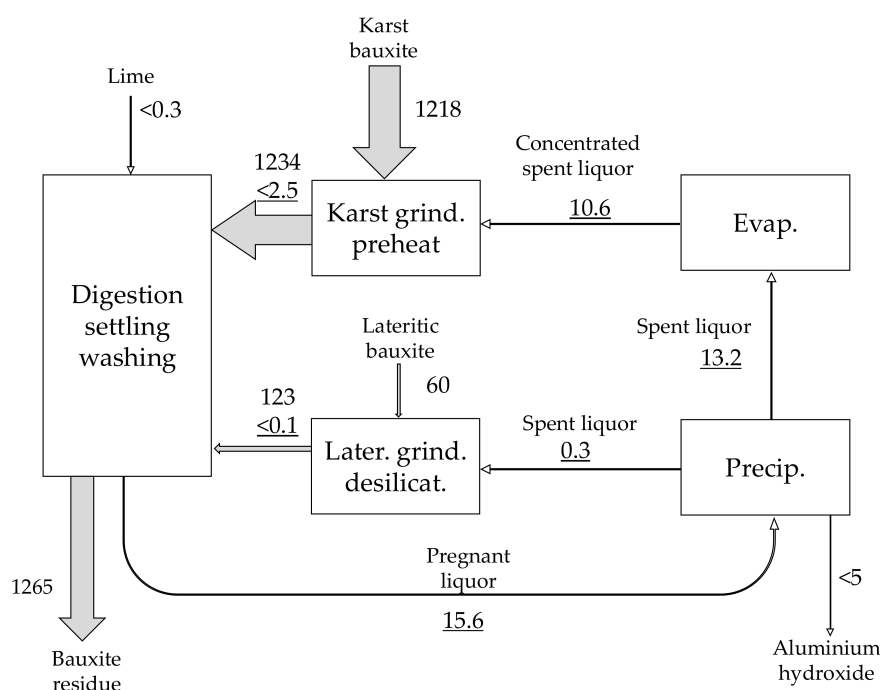


**Figure 5.** Mass distribution of Cr (mg/kg) normalised to mass of aluminium hydroxide produced, based on ICP-MS (solids and liquors) data.

In the mass balance models of Ga, V, As and Cr it can be noted that during the “karst bauxite grinding and preheating” as well as in smaller scale during “lateritic bauxite desilication”, a pronounced increase in trace element concentration is observed in the solid fraction flows. This increase of trace constituents is occurring with the simultaneous decrease in concentrations in liquid flows. Thus, the trace constituents appear to precipitate during these processing phases. Probably, the trace elements precipitate in the composition of Bayer process characteristic solid phases, that are a group of Ca-, Al-, Na- and Si-containing phases, including desilication products (sodalite and cancrinite), hydrogarnet (hydrogrossular) type phases as well as calcium titanate in the form of perovskite ( $\text{CaTiO}_3$ ) [42,73]. Calcium vanadate or  $\text{Ca}_3\text{Al}_2(\text{OH})_{12}$  are already known species that contain V in Bayer process-specific solid phases [71,73]. As mentioned before, lime addition position on the schemes is a simplification and it is added in more processing steps, including the preheating,

thus the possibility of forming Ca-containing species is not limited to the digestion stage. Therefore, during the preheating stage, the trace elements occurring in the spent liquor (Ga, V, As and Cr) are thought to precipitate in the composition of Bayer process characteristic solid phases. While this effect occurs, the trace element concentration in the liquid fraction decreases and in the solid fraction increases. At the same time, the mass balance equilibrium of the trace elements is maintained. During digestion, the pregnant process liquor becomes saturated again in the trace elements on the account of leaching of the newly added bauxite feed.

Another characteristic that can be observed from the mass distributions of Ga, V, As and Cr is that their product-normalised content shows a decreasing trend from pregnant liquor to spent liquor and then to concentrated spent liquor. Only for Ga it is evident that part of its mass is removed from the liquor during precipitation. Since it is observed in the distribution patterns of all the named trace elements, it can be concluded being a systematic behaviour. The working hypothesis is that minor deposition of the trace constituents occurs throughout the mentioned production steps in the form of secondary precipitates or solid formations like scales in the cooler parts of piping or in the solids of filter cakes (e.g., from security filtration of pregnant liquor, “liquor polishing”) [10,44,47]. As already mentioned, some trace elements (Y, Nb, Zr) have been detected in perovskite-based scales in the Bayer circuit [76]. Enhanced concentrations of trace elements like Ni, Cr and V in the range of 700–4900 mg/kg were detected in perovskite-dominated matrix of a scale sample formed in the AoG’s digestion autoclave. The cancrinite-dominated matrix of the same sample was, however, relatively depleted in trace elements (e.g., 140–170 mg/kg V) [77]. Sometimes, enhanced concentrations of V (112 mg/kg) and Ga (28 mg/kg) have been identified in the alumina dust from calciner electrostatic filters, making this material an attractive source of V and Ga [78]. The former examples therefore support the hypothesis that a proportion of trace elements is deposited to minor by-products of the Bayer process. Scales, filter cakes and electrostatic filter dust are regularly cleaned during the production. The volumes of these materials being created are not easily quantifiable, but an assumption can be made that the decrease in the trace element concentrations in the liquor stream can account to the passing of the trace elements to the formerly mentioned minor by-products of the Bayer process as result of the described systematic behaviour.

For the previously discussed elements (Ga, V, As and Cr), it can be concluded that they first accumulate to Bayer process liquor (although Cr in very small extent) and once their saturation level in liquor is achieved, their input and output flows equilibrate. Minor output of those trace elements probably occurs into minor Bayer process by-products from the liquor-based circuit as the concentrations in liquors drop systematically in the consecutive production steps.

### 3.2. Metals that Do Not Accumulate to Liquor

Cerium (Ce) distribution is presented as the representative of LREE elements due to its highest concentration in analysed materials and good analytical stability (Figure 6, Supplementary Table S2). The rest of the mass balances of REEs can be found in Supplementary Table S5 (based on ICP-MS data) and Table S6 (based on INAA data). The input of Ce from lateritic bauxite is practically insignificant and almost the sole source of it is karst bauxite (99%). Cerium distribution is dictated by solid materials only. On the “white side” of the Bayer process, all the analysed concentrations of Ce are below detection limits (aluminium hydroxide < 3 mg/kg, process liquors < 0.04 mg/kg). Ce content remains steady from bauxite to intermediate suspension solid fraction and then to bauxite residue. In the end of the process, there is only one percent difference in the input and output quantities.

The distribution of Y is presented as the representative of HREEs given its highest concentration among this group of elements (Figure 7). Except for the quantities, the distribution of Y is identical to the one of Ce. In all processing stages, its distribution follows the solid materials and Y does not dissolve in the process liquor and thus does not enter into aluminium hydroxide product. The difference in the quantity of input and output of Y (four percent) is higher than for most of the REEs, but still acceptable for presenting its mass balance model.

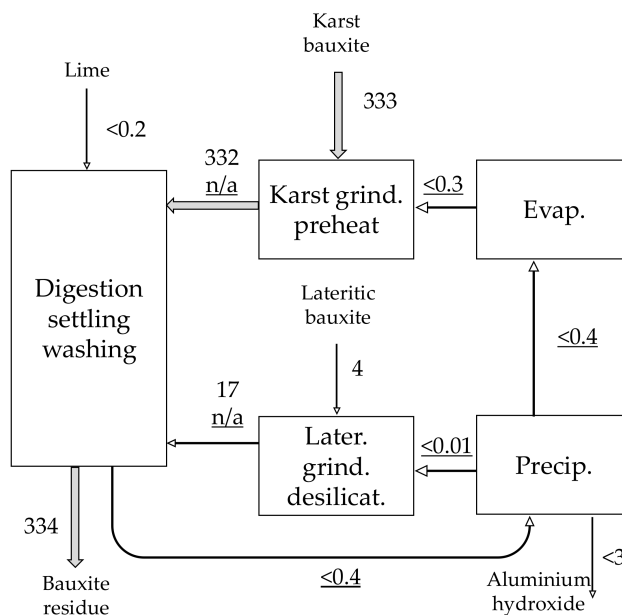


**Figure 6.** Mass distribution of Ce (mg/kg) normalised to mass of aluminium hydroxide produced, based on INAA (solids) and ICP-MS (liquors) data.

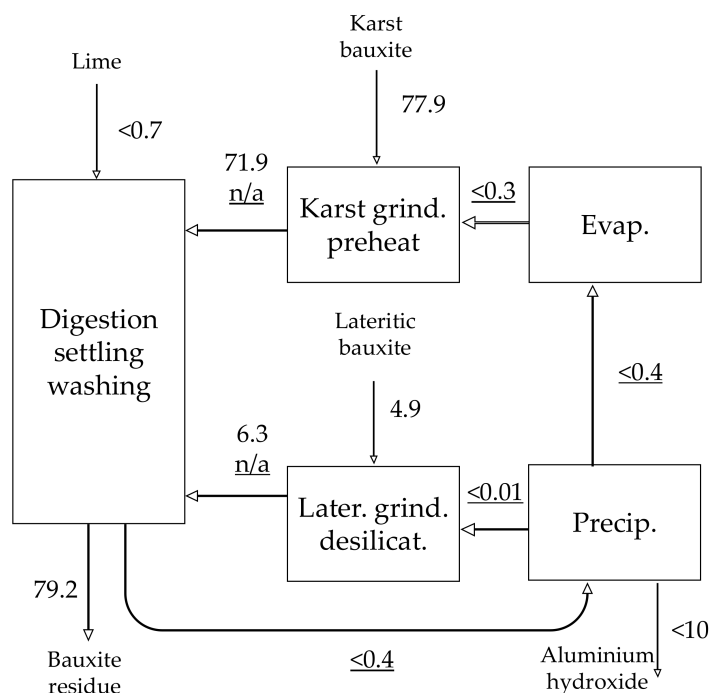


**Figure 7.** Mass distribution of Y (mg/kg) normalised to mass of aluminium hydroxide produced, based on ICP-MS (solids and liquors).

Finally, the distribution of Sc is presented in Figure 8. Note that the quantities of Sc were analysed by INAA method. The majority of Sc originates from karst bauxite source (96%).

Suss et al. report that Sc is expected to occur in a dissolved form during Bayer digestion, but, it probably precipitates rapidly in an unknown form that might be  $ScO(OH)$  or  $Sc(OH)_3$  [13]. The progression of Sc through the process is once more regulated by solid material matrix from bauxite to intermediate solids and then to residue. There is no missing quantity of Sc throughout the processing. The present result is slightly different from the previous results of Sc distribution patterns, where

0.6–1.5 mg/kg bauxite-feed-normalised concentration of Sc was detected in aluminium hydroxide products in Alumina Plant of Urals and Bogoslovski Alumina Plant [25]. It can be noted, though, that the processing conditions between the Russian alumina plants and AoG are different, since the former also partly included sintering of the bauxite ore, although it was not performed for the total amount of bauxite feed.

For most the REEs as well as for Sc distribution, a deficiency in the mass balance in the output of limestone separation HMS unit is noted. This can be regarded as a problem of material representativeness. However, since this is a pre-processing step, it does not affect the mass balance models of the Bayer process.

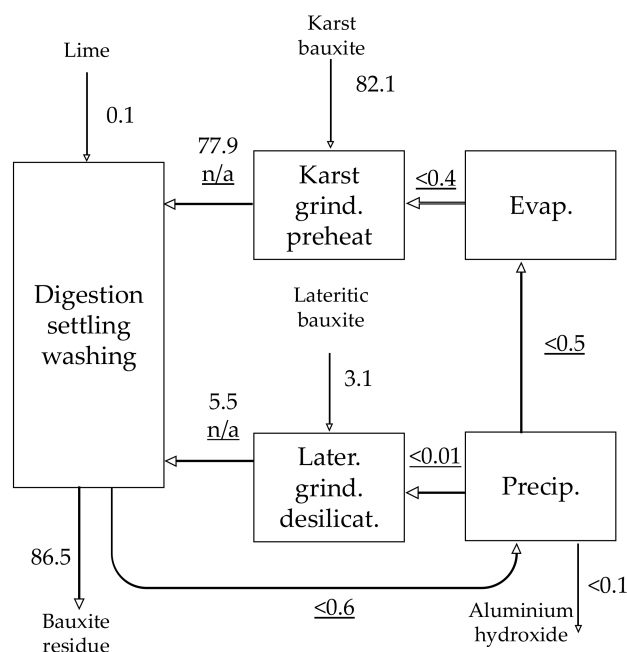


**Figure 8.** Mass distribution of Sc (mg/kg) normalised to mass of aluminium hydroxide produced, based on INAA (solids and liquors).

Besides the REEs distribution presented graphically (Figures 6–8), all the mass balance inventories of the REEs (except for Tb, Ho and Tm due to low concentrations) are available in the compiled dataset (Supplementary Tables S5 and S6). Even lutetium (Lu), the last chemical element in the lanthanides group, mass balance was possible to be quantified given the very low detection limit (0.05 mg/kg) available in INAA method for this element. The data shows consistently that all the analysed REEs behave similarly during bauxite processing and at least 95% of the REEs entering into Bayer process are transferred in the composition of solid matrix to bauxite residue. Furthermore, in most of cases the transfer rate of REEs to bauxite residue is more than 98%. None of the REEs or Sc enter into aluminium hydroxide, given the available detection limits, e.g., La < 0.5 mg/kg, Sm < 0.1 mg/kg or Sc < 0.1 mg/kg (Supplementary Table S2). The fact that REEs and Sc are transferred to bauxite residue only in the composition of solid material is also supported by mineralogical studies [60,77]. One of the investigations has shown that the form of Sc occurrence mainly in the composition of hematite remains the same after bauxite processing [77]. On the other hand, the precursor REE phases found in bauxite are affected by the Bayer process conditions and REE ferrotitanate type compounds are created, but the transformations taking place seem to occur in situ on mineral grain surfaces without the dissolution of the precursor REE phases [60]. Present case study was not able to repeat the result that up to five percent of total La content can be passed to aluminium hydroxide product [25]. This difference can be again explained by the differences between the operational conditions of refineries, as mentioned above. It can be noted, however, that low La presence has been semi-quantitatively found in some

2 w/v% aluminium hydroxide suspensions (Chemtrade Rehydrigel<sup>®</sup> LV and SPI Pharma Aluminum hydroxide wetgel VAC 20; 0.14 and 0.72 mg/L La, respectively) that are used as adjuvants in vaccines by applying very sensitive ICP-MS techniques. At the same time, the concentrations of Ce, Nd and Sc were below detection limits, <0.0005, <0.002 and <0.01 mg/L, respectively [79].

Inconsistencies in the mass balance of some REEs such as Ce can be noted in the “lateritic bauxite grinding and desilication” unit (Figure 6). Such situation is best explained with the possibility that during sampling, some contribution of the other lateritic bauxite from Ghana was also present in the lateritic bauxite slurry. Presently sampled Ghanaian bauxite contains higher concentration of REEs and Sc compared to the existing Brazilian bauxite and by hypothetically replacing the two bauxites in the mass balance calculation resolves the inconsistency. However, in a broad sense this discrepancy is not an issue because the total input and output flows are well within acceptable balance and besides, the input of REEs and Sc from lateritic bauxites has a minor magnitude regardless of the two lateritic bauxite types.

### 3.3. Fractionation Indexes and Systemic Predictions

All the analysed elements except for Ga are enriched in the bauxite residue. This can be emphasised by calculating the fractionation indexes by dividing trace element concentration in bauxite residue with the same parameter in bauxite feed (Figure 9). The fractionation indexes of all the elements except for Ga are like the (1) ratio of bauxite feed mass to bauxite residue mass created during sampling period (2.33), (2) fractionation index of Fe<sub>2</sub>O<sub>3</sub> during sampling period (2.34), and (3) fractionation index of Fe<sub>2</sub>O<sub>3</sub> during one-year period (2.31). Iron oxide fractionation index is considered for a comparison here because it represents a largely inert oxide in the Bayer process, as well as because it has been used for a similar comparison before [29]. All the indexes of trace elements (except Ga) differ from the three major indexes by a maximum of six percent and for most cases less than two percent. The differences are essentially negligible and probably account for errors in sample representativeness and/or analytical variations. This similarity of indexes is well-reasoned, because raw-material-to-residue ratio or Fe<sub>2</sub>O<sub>3</sub> fractionation index set a logical boundary, what can be the maximum possible fractionation index of a constituent in the process. Basically, new material cannot be created during the process and if the constituent does not fractionate to aluminium hydroxide product, then the fractionation index must be like the one for Fe<sub>2</sub>O<sub>3</sub> or the bauxite-feed-to-residue coefficient. Present result is similar to what was concluded in lab-scale testing of trace element enrichment from bauxite to bauxite residue, although higher variations were noted in lab testing [29].

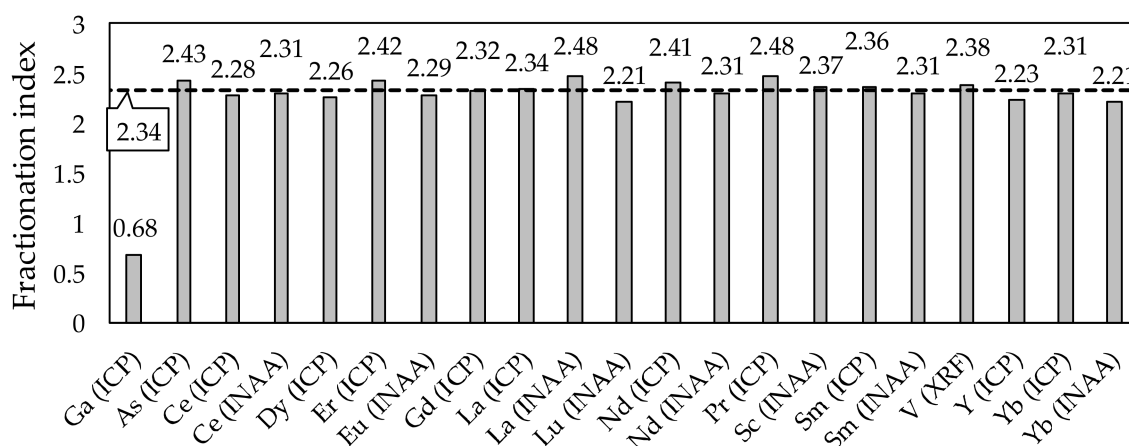


**Figure 9.** Fractionation indexes of trace elements calculated as trace element concentration in bauxite residue divided by trace element concentration in bauxite. Fractionation indexes are compared to the one of Fe<sub>2</sub>O<sub>3</sub> during sampling period (horizontal dashed line).

The former reasoning provides opportunities for predicting the trace element concentrations in bauxite residue based on existing information about bauxite feed. First option is based on  $\text{Fe}_2\text{O}_3$  concentration in bauxite and bauxite residue, as shown in Equation (3). It is not uncommon that the conditionally inert  $\text{Fe}_2\text{O}_3$  is used as an aid in mass balance estimations relating to the Bayer process [80].

$$C_{\text{BR}} = \frac{C_{\text{Fe-BR}}}{C_{\text{Fe-BX}}} \times C_{\text{BX}}, \quad (3)$$

where:

$C_{\text{BR}}$ : Predicted concentration of trace element in bauxite residue, mg/kg;

$C_{\text{Fe-BR}}$ :  $\text{Fe}_2\text{O}_3$  concentration in bauxite residue, %;

$C_{\text{Fe-BX}}$ :  $\text{Fe}_2\text{O}_3$  concentration in bauxite, %;

$C_{\text{BX}}$ : Average concentration of trace element in bauxite feed, mg/kg.

Another option is to consider just the mass flows of bauxite feed and resulting residue created, as shown in Equation (4) and combine it with trace element concentration in bauxite feed. In any case, care must be taken on the representativeness of the bauxite trace element concentration values, because considerably high variations can occur in some bauxite deposits [27].

$$C_{\text{BR}} = \frac{M_{\text{tot-BX}}}{M_{\text{tot-BR}}} \times C_{\text{BX}}, \quad (4)$$

where:

$C_{\text{BR}}$ : Predicted concentration of trace element in bauxite residue, mg/kg;

$M_{\text{tot-BX}}$ : Total dry mass of bauxite fed into system, kg;

$M_{\text{tot-BR}}$ : Total dry mass of bauxite residue leaving the system, kg;

$C_{\text{BX}}$ : Average concentration of trace element in bauxite feed, mg/kg.

Equations (3) and (4) can be used only for the trace elements which do not fraction to aluminium hydroxide product, therefore it is not applicable for such metals as Ga.

#### 4. Conclusions

Bauxite trace elements under the Bayer process extraction conditions and the types of bauxite used in this study are roughly divided in two categories: (1) those that are at least partly soluble in the caustic leaching and accumulate to an extent into process liquor, namely Ga, V, As as well as Cr, and (2) those that are not soluble in the caustic leaching, namely Sc, and the REEs. The trace elements in the first category accumulate in the process liquor until the specific saturation level of each metal, and then the input and output flows equilibrate. In the Bayer process output flows, only Ga possesses the property of entering into the composition of aluminium hydroxide product to the extent of 70% of total Ga output mass. The rest of the Ga is separated from the process with bauxite residue. With respect to the second category, those metals (Sc, REEs) are transferred through the process only in the composition of solid material flows. Sc and REEs are not found in the aluminium hydroxide product and their mass transfer to bauxite residue is mostly at least 98%.

It is evident that Bayer process materials, whether they are bauxite residue or process liquors, are enriched in certain trace elements. Together with the continuous development and improvement of extraction technologies, the trace elements could be recovered as valuable by-products of the Bayer process.

**Supplementary Materials:** The following are available online at <http://www.mdpi.com/2075-4701/8/5/327/s1>, Supplementary file containing Table S1: main element composition of sampled solid materials, Table S2: trace element composition of sampled solid materials, Table S3: composition of Bayer liquors, Table S4: mass distribution of metals (and metalloids) that accumulate to process liquor, Table S5: mass distribution of trace elements that do

not accumulate to process liquors, based on ICP-MS data, Table S6: mass distribution of trace elements that do not accumulate to process liquors, based on INAA data.

**Author Contributions:** J.V., V.V. and D.P. conceived and designed the experiments; J.V. prepared the materials and A.A. performed the experiments; J.V. and D.P. analysed the data; V.V. contributed the reagents and materials; J.V. wrote the paper; D.P. and A.A. contributed to the writing of the paper.

**Acknowledgments:** Athina Filippou and her team of chemical analysts in AoG are thanked for their valuable help in several analytical tasks. The help of Sokratis Tekidis with material mass flow data and sample collection is greatly appreciated. György (George) Bánvölgyi and Ken Evans are kindly acknowledged for their invaluable support throughout the project. The research leading to these results has received funding from the European Community's Horizon 2020 Programme (H2020/2014–2019) under Grant Agreement no. 636876 (MSCA-ETN REDMUD). This publication reflects only the authors' views, exempting the Community from any liability. Project website: <http://www.etn.redmud.org>.

**Conflicts of Interest:** The authors declare no conflict of interest.

## References

1. Binnemans, K.; Jones, P.T.; Müller, T.; Yurramendi, L. Rare Earths and the Balance Problem: How to Deal with Changing Markets? *J. Sustain. Metall.* **2018**, *4*, 126–146. [[CrossRef](#)]
2. Christmann, P.; Arvanitidis, N.; Martins, L.; Recoché, G.; Solar, S. Towards the Sustainable Use of Mineral Resources: A European Geological Surveys Perspective. *Miner. Energy Raw Mater. Rep.* **2007**, *22*, 88–104. [[CrossRef](#)]
3. Christmann, P. Towards a More Equitable Use of Mineral Resources. *Nat. Resour. Res.* **2018**, *27*, 159–177. [[CrossRef](#)]
4. European Commission; Deloitte Sustainability; TNO; British Geological Survey; Bureau de Recherches Géologiques et Minières. *Study on the Review of the List of Critical Raw Materials*; Publications Office of the European Union: Luxembourg, 2017; pp. 1–93.
5. Balomenos, E.; Davris, P.; Dedy, E.; Yang, J.; Panias, D.; Friedrich, B.; Binnemans, K.; Seisenbaeva, G.; Dittrich, C.; Kalvig, P.; et al. The EURARE Project: Development of a Sustainable Exploitation Scheme for Europe's Rare Earth Ore Deposits. *Johns. Matthey Technol. Rev.* **2017**, *61*, 142–153. [[CrossRef](#)]
6. Davris, P.; Balomenos, E.; Taxiarchou, M.; Panias, D.; Paspaliaris, I. Current and Alternative Routes in the Production of Rare Earth Elements. *Berg. Huetttenmaenn. Monatsh.* **2017**, *162*, 245–251. [[CrossRef](#)]
7. Evans, K. The history, challenges, and new developments in the management and use of bauxite residue. *J. Sustain. Metall.* **2016**, *2*, 316–331. [[CrossRef](#)]
8. Frenzel, M.; Ketris, M.P.; Seifert, T.; Gutzmer, J. On the current and future availability of gallium. *Resour. Policy* **2016**, *47*, 38–50. [[CrossRef](#)]
9. Authier-Martin, M.; Forte, G.; Ostap, S.; See, J. The mineralogy of bauxite for producing smelter-grade alumina. *JOM* **2001**, *53*, 36–40. [[CrossRef](#)]
10. Teas, E.B.; Kotte, J.J. The effect of impurities on process efficiency and methods for impurity control and removal. In Proceedings of the JBI-JGS Symposium Titled "Bauxite/Alumina Industry in the Americas", Kingston, Jamaica, 1980; Volume 23, pp. 100–129.
11. Davris, P.; Balomenos, E.; Panias, D.; Paspaliaris, I. Selective leaching of rare earth elements from bauxite residue (red mud), using a functionalized hydrophobic ionic liquid. *Hydrometallurgy* **2016**, *164*, 125–135. [[CrossRef](#)]
12. Hudson, L.K. Gallium as a by-product of alumina manufacture. *J. Met.* **1965**, *17*, 948–951. [[CrossRef](#)]
13. Suss, A.; Kuznetsova, N.V.; Kozyrev, A.; Panov, A.; Gorbachev, S. Specific features of scandium behavior during sodium bicarbonate digestion of red mud. In Proceedings of the 35th International ICSOBA Conference, Hamburg, Germany, 2–5 October 2017; Volume 42, pp. 491–504.
14. Suss, A.; Paromova, I.; Panov, A.; Shipova, O.V.; Kutkova, N.N. Behaviour of Beryllium in Alumina Production from Bauxites by Bayer Process and Development of Reliable Method of Its Determination. In Proceedings of the Light Metals Conference, New Orleans, LA, USA, 9–12 March 2008; pp. 107–112.
15. Løvik, A.N.; Restrepo, E.; Müller, D.B. The global anthropogenic gallium system: Determinants of demand, supply and efficiency improvements. *Environ. Sci. Technol.* **2015**, *49*, 5704–5712. [[CrossRef](#)] [[PubMed](#)]
16. Pradhan, R.J.; Das, S.N.; Thakur, R.S. Vanadium sludge—An useful byproduct of alumina plant. *J. Sci. Ind. Res.* **1999**, *58*, 948–953.

17. Binnemans, K.; Jones, P.T.; Blanpain, B.; Van Gerven, T.; Pontikes, Y. Towards zero-waste valorisation of rare-earth-containing industrial process residues: A critical review. *J. Clean. Prod.* **2015**, *99*, 17–38. [[CrossRef](#)]
18. Borra, C.R.; Blanpain, B.; Pontikes, Y.; Binnemans, K.; Van Gerven, T. Recovery of rare earths and other valuable metals from bauxite residue (red mud): A review. *J. Sustain. Metall.* **2016**, *2*, 365–386. [[CrossRef](#)]
19. Atwood, D.A. *The Rare Earth Elements: Fundamentals and Applications*; John Wiley & Sons: Lexington, KY, USA, 2012; ISBN 978-1-119-95097-4.
20. Gray, F.; Kramer, D.A.; Bliss, J.D. Gallium and gallium compounds. In *Kirk-Othmer Encyclopedia of Chemical Technology*; John Wiley & Sons, Inc.: Hoboken, NJ, USA, 2013. [[CrossRef](#)]
21. Bauer, G.; Güther, V.; Hess, H.; Otto, A.; Roidl, O.; Roller, H.; Sattelberger, S.; Köther-Becker, S.; Beyer, T.; Bauer, G.; et al. Vanadium and Vanadium Compounds. In *Ullmann's Encyclopedia of Industrial Chemistry*; John Wiley & Sons: Hoboken, NJ, USA, 2017; ISBN 978-3-527-30673-2.
22. Wang, W.; Pranolo, Y.; Cheng, C.Y. Metallurgical processes for scandium recovery from various resources: A review. *Hydrometallurgy* **2011**, *108*, 100–108. [[CrossRef](#)]
23. Habashi, F. Gallium update. In Proceedings of the 17th International Symposium ICSOBA, Montréal, QC, Canada, 1–4 October 2006; Volume 33, pp. 141–153.
24. Deady, É.A.; Mouchos, E.; Goodenough, K.; Williamson, B.J.; Wall, F. A review of the potential for rare-earth element resources from European red muds: Examples from Seydişehir, Turkey and Parnassus-Giona, Greece. *Mineral. Mag.* **2016**, *80*, 43–61. [[CrossRef](#)]
25. Derevyankin, V.A.; Porotnikova, T.P.; Kocherova, E.K.; Yumasheva, I.V.; Moiseev, V.E. Behaviour of scandium and lanthanum in the production of alumina from bauxite (in Russian). *Izvestiya Vysshikh Uchebnykh Zavedenii Tsvetnaya Metallurgiya* **1981**, *4*, 86–89.
26. Mohapatra, B.K.; Mishra, B.K.; Mishra, C.R. Studies on metal flow from khondalite to bauxite to alumina and rejects from an alumina refinery, India. In *Light Metals*; Suarez, C.E., Ed.; John Wiley & Sons, Inc.: Hoboken, NJ, USA, 2012; pp. 87–91. ISBN 978-1-118-35925-9.
27. Ochsenkühn-Petropulu, M.; Lyberopulu, T.; Parissakis, G. Direct determination of lanthanides, yttrium and scandium in bauxites and red mud from alumina production. *Anal. Chim. Acta* **1994**, *296*, 305–313. [[CrossRef](#)]
28. Wagh, A.S.; Pinnock, W.R. Occurrence of scandium and rare earth elements in Jamaican bauxite waste. *Econom. Geol.* **1987**, *82*, 757–761. [[CrossRef](#)]
29. Feret, F.R.; See, J. A comparative study of analytical methods of trace elements in bauxite and red mud. In Proceedings of the 18th International Symposium ICSOBA Travaux, Zhengzhou, China, 25–28 November 2010; pp. 68–83.
30. Logomerac, V.G. Distribution of rare-earth and minor elements in some bauxite and red mud produced. In Proceedings of the Second International Symposium of ICSOBA, Budapest, Hungary, 6–10 October 1969; Volume 3, pp. 383–393.
31. Papp, E.; Zsindely, S.; Tomcsanyi, L. Molybdenum and zinc traces in the Bayer process. In Proceedings of the 2nd International Symposium ICSOBA, Budapest, Hungary, 6–10 October 1969; Volume 3, pp. 395–402.
32. Eyer, S.; Nunes, M.; Dobbs, C.; Russo, A.; Burke, K. The analysis of beryllium in Bayer solids and liquids. In Proceedings of the 7th International Alumina Quality Workshop, Perth, Australia, 16–21 October 2005; Volume 1, pp. 254–257.
33. Sato, C.; Kazama, S.; Sakamoto, A.; Hirayanagi, K. Behavior of radioactive elements (uranium and thorium) in Bayer process. In *Reprinted in Essential Readings in Light Metals*; Donaldson, D., Raahauge, B.E., Eds.; John Wiley & Sons, Inc.: Hoboken, NJ, USA, 2013; pp. 191–197. ISBN 978-1-118-64786-8.
34. Bansal, N.; Vaughan, J.; Tam Wai Yin, P.; Leong, T.; Boulemant, A. Chemical thermodynamics of mercury in the Bayer process. In Proceedings of the 7th International Symposium on Hydrometallurgy (Hydro2014), Victoria, BC, Canada, 22–25 June 2014; Volume II, pp. 559–569.
35. Bansal, N.; Vaughan, J.; Boulemant, A.; Leong, T. Determination of total mercury in bauxite and bauxite residue by flow injection cold vapour atomic absorption spectrometry. *Microchem. J.* **2014**, *113*, 36–41. [[CrossRef](#)]
36. Bárdossy, G. *Karst Bauxites: Bauxite Deposits on Carbonate Rocks*; Developments in Economic Geology 14; Elsevier Scientific Pub. Co.: Amsterdam, The Netherlands, 1982; ISBN 978-0-444-99727-2.
37. Valetton, I. *Bauxites*; Developments in Soil Science 1; Elsevier Publishing Company: Amsterdam, The Netherlands, 1972; ISBN 978-0-444-40888-4.

38. Adamson, A.N.; Bloore, E.J.; Carr, A.R. Basic Principles of Bayer Process Design. In *Reprinted in Essential Readings in Light Metals*; Donaldson, D., Raahauge, B.E., Eds.; John Wiley & Sons, Inc.: Hoboken, NJ, USA, 2013; pp. 100–117. ISBN 978-1-118-64786-8.
39. Chin, L.A.D. The state-of-the-art in Bayer process technology. *Light Met.* **1988**, *1988*, 49–53.
40. Power, G.; Gräfe, M.; Klauber, C. Bauxite residue issues: I. Current management, disposal and storage practices. *Hydrometallurgy* **2011**, *108*, 33–45. [[CrossRef](#)]
41. S&P Global Platts, a Division of S&P Global Inc. Methodology and Specifications Guide, Nonferrous. Available online: <https://www.platts.com/methodology-specifications/metals> (accessed on 3 March 2018).
42. Gräfe, M.; Power, G.; Klauber, C. Bauxite residue issues: III. Alkalinity and associated chemistry. *Hydrometallurgy* **2011**, *108*, 60–79. [[CrossRef](#)]
43. Hudson, L.K.; Misra, C.; Perrotta, A.J.; Wefers, K.; Williams, F.S. Aluminum Oxide. In *Ullmann's Encyclopedia of Industrial Chemistry*; Wiley-VCH Verlag GmbH & Co.: Weinheim, Germany, 2000; Volume 2, pp. 607–645. ISBN 978-3-527-30673-2.
44. Lavalou, E.; Bosca, B.; Keramidis, O. Alumina production from diasporic bauxites. *Light Met.* **1999**, CD-ROM Collection, 55–62.
45. Papanastassiou, D.; Contaroudas, D.; Solymár, K. Processing and marketing of Greek diasporic bauxite for metallurgical and non-metallurgical applications. In Proceedings of the 17th International Symposium of ICSOBA, “Aluminium: From Raw Materials to Applications”, Montréal, QC, Canada, 1–4 October 2006.
46. Whittington, B.I. The chemistry of CaO and Ca(OH)<sub>2</sub> relating to the Bayer process. *Hydrometallurgy* **1996**, *43*, 13–35. [[CrossRef](#)]
47. Bánvölgyi, G. Scale formation in alumina refineries. In Proceedings of the 34th International Conference and Exhibition ICSOBA, Quebec, QC, Canada, 3–6 October 2016; pp. 1–14.
48. Laskou, M.; Economou-Eliopoulos, M. The role of microorganisms on the mineralogical and geochemical characteristics of the Parnassos-Ghiona bauxite deposits, Greece. *J. Geochem. Explor.* **2007**, *93*, 67–77. [[CrossRef](#)]
49. Boulangé, B.; Carvalho, A. The bauxite of Porto Trombetas. In *Brazilian Bauxites*; Carvalho, A., Boulangé, B., Melfi, A.J., Lucas, Y., Eds.; NUPEGEL, Departamento de Geologia Geral Universidade de Sao Paulo, Brasil: São Paulo, Brazil, 1997.
50. Adam, C.; Krüger, O. Challenges in analysing rare earth elements in different waste matrices to determine recovery potentials. In *Book of Abstracts, 2nd Conference on European Rare Earth Resources*; Heliotopos Conferences Ltd.: Santorini, Greece, 2017; pp. 237–239.
51. Ochsenkühn-Petropoulou, M.; Ochsenkühn, K.; Luck, J. Comparison of inductively coupled plasma mass spectrometry with inductively coupled plasma atomic emission spectrometry and instrumental neutron activation analysis for the determination of rare earth elements in Greek bauxites. *Spectrochim. Acta Part B At. Spectrosc.* **1991**, *46*, 51–65. [[CrossRef](#)]
52. Hoffman, E.L. Instrumental neutron activation in geoanalysis. *J. Geochem. Explor.* **1992**, *44*, 297–319. [[CrossRef](#)]
53. Govindaraju, K. Report (1967–1981) on four ANRT rock reference samples: Diorite DR-N, serpentine UB-N, bauxite BX-N and disthene DT-N. *Geostand. Newsl.* **1982**, *6*, 91–159. [[CrossRef](#)]
54. Govindaraju, K.; Roelandts, I. 1988 compilation report on trace elements in six ANRT rock reference samples: Diorite DR-N, serpentine UB-N, bauxite BX-N, disthene DT-N, granite GS-N and potash feldspar FK-N. *Geostand. Geoanal. Res.* **1989**, *13*, 5–67. [[CrossRef](#)]
55. Singh, U.; Mishra, R.S. Simultaneous multielemental analysis of alumina process samples using inductively coupled plasma spectrometry (ICP-AES). *Anal. Chem. Indian J.* **2012**, *11*, 1–5.
56. Yamada, Y. X-ray fluorescence analysis by fusion bead method for ores and rocks. *Rigaku J.* **2010**, *26*, 15–23.
57. Metrohm, Determination of Total Caustic, Total Soda and Alumina in Bayer Process Liquors with 859 Titrotherm. Available online: [http://partners.metrohm.com/GetDocument?action=get\\_dms\\_document&docid=693348](http://partners.metrohm.com/GetDocument?action=get_dms_document&docid=693348) (accessed on 23 March 2018).
58. Brookins, D.G. *Eh-pH Diagrams for Geochemistry*; Springer Science & Business Media: Berlin/Heidelberg, Germany, 1988; ISBN 978-3-642-73093-1.
59. Brookins, D.G. Eh-pH diagrams for the rare earth elements at 25 C and one bar pressure. *Geochem. J.* **1983**, *17*, 223–229. [[CrossRef](#)]

60. Vind, J.; Malfliet, A.; Blanpain, B.; Tsakiridis, P.E.; Tkaczyk, A.H.; Vassiliadou, V.; Panias, D. Rare Earth Element Phases in Bauxite Residue. *Minerals* **2018**, *8*, 77. [[CrossRef](#)]
61. Gamaletsos, P.N. Mineralogy and Geochemistry of Bauxites from Parnassos-Ghiona Mines and the Impact on the Origin of the Deposits. Ph.D. Thesis, National and Kapodistrian University of Athens, Athens, Greece, 2014.
62. Wellington, M.; Valcin, F. Impact of Bayer Process Liquor Impurities on Causticization. *Ind. Eng. Chem. Res.* **2007**, *46*, 5094–5099. [[CrossRef](#)]
63. Schulte, R.F.; Foley, N.K. *Compilation of Gallium Resource Data for Bauxite Deposits*; U.S. Geological Survey: Reston, VA, USA, 2014. [[CrossRef](#)]
64. Shaw, D.M. The geochemistry of gallium, indium, thallium—A review. *Phys. Chem. Earth* **1957**, *2*, 164–211. [[CrossRef](#)]
65. Figueiredo, A.M.G.; Avristcher, W.; Masini, E.A.; Diniz, S.C.; Abrão, A. Determination of lanthanides (La, Ce, Nd, Sm) and other elements in metallic gallium by instrumental neutron activation analysis. *J. Alloys Compd.* **2002**, *344*, 36–39. [[CrossRef](#)]
66. Riveros, P.A. Recovery of gallium from Bayer liquors with an amidoxime resin. *Hydrometallurgy* **1990**, *25*, 1–18. [[CrossRef](#)]
67. Lamerant, J.-M. Process for Extracting and Purifying Gallium from Bayer Liquors. Patent No US5102512 A, 10 April 1991.
68. Lamerant, J.-M. Process for Extracting Gallium from Bayer Liquors Using an Impregnated Absorbent Resin. Patent No. US5424050 A, 13 June 1995.
69. Selvi, P.; Ramasami, M.; Samuel, M.H.P.; Sripriya, R.; Senthilkumar, K.; Adaikkalam, P.; Srinivasan, G.N. Gallium recovery from Bayer's liquor using hydroxamic acid resin. *J. Appl. Polym. Sci.* **2004**, *92*, 847–855. [[CrossRef](#)]
70. Ilić, Z.; Mitrović, A. Determination of gallium in Bayer process sodium aluminate solution by inductively coupled plasma atomic emission spectrometry. *Anal. Chim. Acta* **1989**, *221*, 91–97. [[CrossRef](#)]
71. Zhao, Z.; Long, H.; Li, X.; Fan, Y.; Han, Z. Precipitation of vanadium from Bayer liquor with lime. *Hydrometallurgy* **2012**, *115–116*, 52–56. [[CrossRef](#)]
72. Fenerty, M.J. Production of Fused Alumina. Patent No. US2961296 A, 22 November 1960.
73. Smith, P. Reactions of lime under high temperature Bayer digestion conditions. *Hydrometallurgy* **2017**, *170*, 16–23. [[CrossRef](#)]
74. Okudan, M.D.; Akcil, A.; Tuncuk, A.; Deveci, H. Effect of parameters on vanadium recovery from by-products of the Bayer process. *Hydrometallurgy* **2015**, *152*, 76–83. [[CrossRef](#)]
75. Burke, I.T.; Mayes, W.M.; Peacock, C.L.; Brown, A.P.; Jarvis, A.P.; Gruiz, K. Speciation of Arsenic, Chromium, and Vanadium in Red Mud Samples from the Ajka Spill Site, Hungary. *Environ. Sci. Technol.* **2012**, *46*, 3085–3092. [[CrossRef](#)] [[PubMed](#)]
76. Zhong-Lin, Y.; Song-Qing, G. Development of research on the scaling problem in Bayer process. *Light Met.* **1995**, 155–159.
77. Vind, J.; Malfliet, A.; Bonomi, C.; Paiste, P.; Sajó, I.E.; Blanpain, B.; Tkaczyk, A.H.; Vassiliadou, V.; Panias, D. Modes of occurrences of scandium in Greek bauxite and bauxite residue. *Miner. Eng.* **2018**, *123*, 35–48. [[CrossRef](#)]
78. Gladyshev, S.V.; Akcil, A.; Abdulvaliyev, R.A.; Tastanov, E.A.; Beisembekova, K.O.; Temirova, S.S.; Deveci, H. Recovery of vanadium and gallium from solid waste by-products of Bayer process. *Miner. Eng.* **2015**, *74*, 91–98. [[CrossRef](#)]
79. Schlegl, R.; Weber, M.; Wruss, J.; Low, D.; Queen, K.; Stilwell, S.; Lindblad, E.B.; Möhlen, M. Influence of elemental impurities in aluminum hydroxide adjuvant on the stability of inactivated Japanese Encephalitis vaccine, IXIARO®. *Vaccine* **2015**, *33*, 5989–5996. [[CrossRef](#)] [[PubMed](#)]
80. Santana, F.; Tartarotti, F. Alumina recovery estimation through material balance in Alumar refinery. In Proceedings of the 19th International Symposium ICSOBA, Belém, Brazil, 29 October–2 November 2012; pp. 1–6.

